

A de Haas-van Alphen effect study of the Fermi surface of lithium

This article has been downloaded from IOPscience. Please scroll down to see the full text article.

1989 J. Phys.: Condens. Matter 1 6589

(<http://iopscience.iop.org/0953-8984/1/37/007>)

View [the table of contents for this issue](#), or go to the [journal homepage](#) for more

Download details:

IP Address: 171.66.16.93

The article was downloaded on 10/05/2010 at 18:48

Please note that [terms and conditions apply](#).

A de Haas–van Alphen effect study of the Fermi surface of lithium

M B Hunt[†], P H P Reinders[‡] and M Springford[†]

School of Mathematical and Physical Sciences, University of Sussex, Brighton, Sussex BN1 9QH, UK

Received 27 January 1989

Abstract. The de Haas–van Alphen effect is used to study the Fermi surface of BCC lithium. The lithium is in the form of a dispersion of micrometre sized grains embedded in wax in order to suppress the low temperature martensitic transformation. A full characterisation of the lithium Fermi surface geometry is not possible, but the overall distortion in area is found to be $3.00 \pm 0.02\%$, from which the radial distortion is estimated as $4.8 \pm 0.3\%$. These distortions are significantly higher than those found by the many-body density functional calculations of Macdonald and the positron annihilation experiments of Oberli *et al.* We obtain from our measurements a probability distribution of de Haas–van Alphen frequencies over the whole Fermi surface. The cyclotron electron effective mass is measured as $(2.10 \pm 0.06)m_0$. This work is an attempt to improve on the earlier work of Randles and Springford by exploiting the higher magnetic fields (13 T) and lower temperatures (20 mK) now available.

1. Motivation and historical survey

At room temperature, lithium is most stable as a BCC lattice but, as it is cooled through about 72 K, a martensitic structural transition to a highly faulted phase once thought to be HCP and now believed to be a 9R samarium type of structure begins [1, 2]. Transition continues with further cooling until at 4.2 K the fraction of transformed phase typically exceeds 90%. The consequent and so far insuperable difficulty of obtaining at low temperatures a single large and good-quality crystal of lithium, of either phase, has made lithium opaque to the usual Fermi surface probes so that no full characterisation of the Fermi surface geometry has yet been made. In this respect, lithium is now unique among common metals. This is unfortunate as lithium is an ideal test case for band-structure models. It has a particularly simple electronic make-up with only two core electrons and one conduction electron per atom and a Brillouin zone large enough to contain the free-electron Fermi sphere so that tractable, nearly free-electron-type models can be used, at least as a starting point.

All theoretical calculations to date have indicated that the Fermi surface of BCC lithium is a distorted sphere, pushed outwards from the free-electron sphere in the $\langle 110 \rangle$

[†] Present address: H H Wills Physics Laboratory, University of Bristol, Tyndall Avenue, Bristol BS8 1TB, UK.

[‡] Present address: Technical Hochschule Darmstadt, Hochschulstrasse 8, 6100 Darmstadt, Federal Republic of Germany.

directions and inwards in the $\langle 100 \rangle$ directions. All but two calculations [3, 4] envisage a single closed surface. Local models predict distortions in the range 4–7%, while the more recent many-body calculations in [5, 6] in which a non-local electron exchange term is included in the crystal potential agree on substantially smaller distortions in the range 1–3%.

This uncertainty as to the *overall distortion* of the Fermi surface is something which experiment can help to resolve, even if it cannot, as yet, map the geometry of the Fermi surface in three dimensions. The experimental evidence prior to 1975, however, based on studies of Compton scattering, positron annihilation and optical properties was contradictory and ambiguous (see [7] for references and a brief review). Since then the situation has been clarified somewhat by two studies, both of which have confirmed the picture of a distorted sphere and shown the maximum Fermi surface distortion to be of the order of 3% which, if true, implies that any realistic model of the BCC lithium Fermi surface must invoke many-body effects.

Most recently, the two-dimensional angular correlation of positron annihilation radiation in a single crystal of BCC lithium at 100 K has been measured [8]. By this means it was possible to include in the analysis the considerable effects of higher-momentum components of the electron wavefunction and to determine the Fermi surface anisotropy throughout the (110) plane. The maximum anisotropy was found to be $2.8 \pm 0.6\%$.

De Haas–van Alphen (DHVA) effect magnetisation oscillations at 1 K in magnetic fields between 9 and 10 T in a colloid of randomly oriented lithium grains embedded in wax were detected and reported in [7]. These grains were between 1 and 100 μm in diameter, with the majority smaller than 10 μm . Low-temperature x-ray studies showed that the martensitic phase transition had been inhibited, so that in [7] oscillations were seen from the BCC phase, assuming that no transition took place between 4.2 and 1 K. Since, in these experiments, all parts of the Fermi surface contributed simultaneously, the Fermi surface geometry could not be mapped out but from the frequency of the prominent beats in the oscillations the overall anisotropy in *extremal cross sectional area* $\Delta\mathcal{A}/\mathcal{A}_0$, where \mathcal{A}_0 is the extremal cross sectional area of the free-electron sphere, could be determined directly. This was related to the maximum radial anisotropy δ , where

$$\delta = (k_{110} - k_{100})/k_0$$

and k_0 is the radius of the free-electron sphere, by generating the DHVA beat structures corresponding to four theoretical models, each with given δ , to find $\Delta\mathcal{A}/\mathcal{A}_0$ for each model. The mean value of $\Delta\mathcal{A}/\mathcal{A}_0$, expressed in terms of the parameter δ , was found to have a small variance, which suggested that $\Delta\mathcal{A}/\mathcal{A}_0$ was a good measure of δ . The models gave $\Delta\mathcal{A}/\mathcal{A}_0 = (0.58 \pm 0.13)\delta$, whilst the experiment gave $\Delta\mathcal{A}/\mathcal{A}_0 = 1.5 \pm 0.3\%$. Thus the best value for δ was deduced from the experiments to be $2.6 \pm 0.9\%$.

The present work attempts the same experiment as in [7] but now at temperatures down to 20 mK and in an extended magnetic field range, up to 13 T. This has enabled a substantially better signal-to-noise ratio and an improved resolution in Fourier analysis of the DHVA oscillations. Resolution is so much better, in fact, that we can deduce the areal anisotropy from the Fourier spectrum itself and can even discern detail within the narrow band of DHVA frequencies deriving from the distorted Fermi surface of lithium.

1.1. Some useful equations

We present here, using the notation in [9], the expression from [10] for the oscillatory part of the magnetisation \tilde{M} of the lithium grains when in an external field H :

$$\tilde{M} = \hat{m}D(H) \sum_{r=1}^{\infty} \frac{\alpha_r(1/H)I_r K_r}{r^{3/2}} \cos(\pi r S) \sin \left[2\pi r \left(\frac{F}{H} - \gamma \right) + p \frac{\pi}{4} \right] \quad (1)$$

where

$$F = \hbar c \mathcal{A} / 2\pi e \quad (2)$$

is the DHVA oscillation frequency and \mathcal{A} is an *extremal* cross sectional area in the plane perpendicular to the applied field. For free electrons, equation (2) becomes

$$F_0 = (\hbar c / 2e) (3\pi^2 N_0)^{2/3}. \quad (3)$$

If we take for the lattice parameter of BCC lithium at 0 K the value given in [7], $a = 3.481 \text{ \AA}$ (see note on p 1834 in [7]), then we obtain $F_0 = 41\,250 \text{ G}$.

In equation (1), we have

$$\hat{m} = [\hat{H} - (1/F)(\partial F / \partial \theta)\hat{\theta} - (1/(F \sin \theta))(\partial F / \partial \varphi)\hat{\varphi}]$$

with $(\hat{H}, \hat{\theta}, \hat{\varphi})$ the unit vectors in the spherical coordinate system defined by the direction of the external magnetic field, i.e.

$$D(H) = -(e\hbar\mathcal{A}/4\pi^4 m_c \mathcal{A}'') (2\pi e H / \hbar)^{1/2} \quad (4)$$

where m_c is the cyclotron effective mass, $\mathcal{A}'' (= |\partial^2 \mathcal{A} / \partial k_H^2|)$ is the curvature of the Fermi surface at the extremal slice and p is $+1$ at a minimum extremal orbit and -1 at a maximum extremal orbit and, in the spin-splitting term $\cos(\pi r S)$,

$$S = (gm_c / 2m_0) \quad (5)$$

where m_0 is the free-electron mass and

$$I_r = (\kappa r m_c^* T / H m_0) / \sinh(\kappa r m_c^* T / H m_0). \quad (6)$$

In this thermal damping term the mass is renormalised by the electron–phonon interaction $m_c^* = m_c(1 + \lambda)$, and

$$\kappa = 2\pi^2 m_0 k_B / e\hbar = 146.9 \text{ kOe K}^{-1}. \quad (7)$$

Also in equation (1),

$$K_r = \exp[-(\kappa r m_c T_D / m_0 H)] \quad (8)$$

where the Dingle temperature T_D is a parametrised orbital average of the electron reciprocal lifetime with the dimension of temperature. We have

$$T_D = (\hbar / 2\pi k_B) \langle 1/\tau \rangle = \Gamma / \pi k_B \quad (9)$$

where Γ is the width of the Lorentzian broadening of the Landau level.

The attenuation parameter $\alpha_r(1/H)$ appears in equation (1) to express the reduction in \tilde{M} that arises from the interference, owing to phase differences, between the DHVA signals from the randomly oriented grains within the sample. It is this interference which causes the observed beat structure. Following [7], we assert that at field H , $\alpha_r(1/H)$ is given by

$$\alpha_r \left(\frac{1}{H} \right) = \left| \int P \left(\frac{F_r}{F_0} \right) \exp \left[\frac{2\pi(F_r - F_0)}{H} \right] \frac{dF_r}{F_0} \right| \quad (10)$$

where F_0 is the free-electron frequency and $P(F/F_0)$ is the normalised distribution DHVA

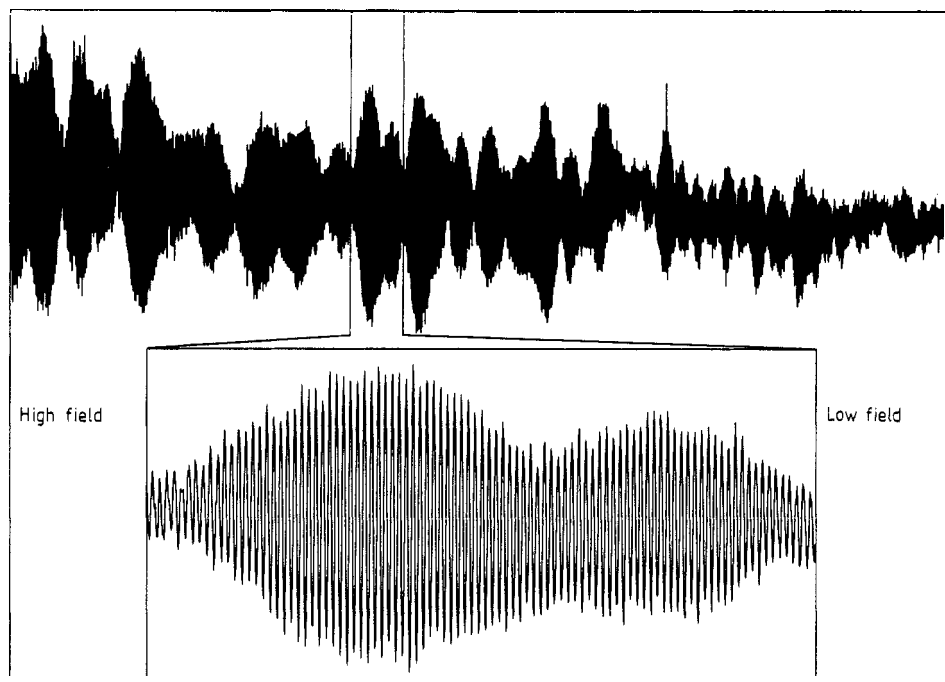


Figure 1. DHVA effect oscillations from a sample of about 2.5×10^6 particles of lithium dispersed in paraffin wax. The full trace, which covers the field range 12.9–7.9 T at a temperature of 20 mK, exhibits a complex beat structure arising from the interference of signals from the randomly oriented particles. The portion of the trace between 11.1 and 10.8 T is shown expanded in the inset.

frequencies over all orientations of the Fermi surface. This result assumes that the grains in the dispersion are perfectly randomly oriented and that there is no variation over the Fermi surface of Dingle temperature, effective mass or g -factor. We shall return to a discussion of this point below in § 3.2.

2. The experiment

For the present work a top-loading dilution refrigerator with attached magnet was used [11], providing a base temperature of 20 mK and a magnetic field up to 13.5 T. The field modulation technique was used, as described in [12], with detection at the second harmonic of the modulation frequency. At the detection frequency of 500 Hz, the skin depth is large in comparison with the diameter of the largest grains (a few hundred micrometres).

The sample was a dispersion of lithium grains (30 vol.%) in wax, and from the same source as that used in the experiment in [7]. It contained an estimated 2.5×10^6 grains of lithium. It was embedded in an unsealed glass capillary of radius 0.55 mm and length 3.0 mm which could be rotated during the experiment about a horizontal axis perpendicular to the magnetic field.

In an experiment, the magnet was normally swept from the top field at $0.000\,68\text{ T s}^{-1}$ while the signal and magnetic field amplitudes were sampled every 0.45 s. This sweep

rate represented the best compromise between noise reduction and human patience. At top field the signal amplitude was, typically, 10 nV at the pick-up coil, while the noise was less than 1 nV in a band width of 0.8 Hz. An estimate of the maximum signal amplitude v_{\max} using equation (1) is in reasonable agreement with that observed. Assuming a mean value of 0.27 for the attenuation parameter in the field range 8–13 T [7] and that $\cos(\pi rS) = 1$ over the whole Fermi surface, then we obtain $v_{\max} \approx 8$ nV.

The cyclotron radius in lithium at a field of 13 T is 0.57 μm . If we assume that, in any grain, an outer shell one cyclotron radius thick does not contribute to the DHVA effect, this means that the DHVA contribution of the smallest grains is very much reduced. The total effective volume of the sample is not much reduced, however, because of the disproportionately large contribution from the larger grains.

The extent of a field sweep depended on the purpose of the experiment. If the purpose was, ultimately, to determine the frequency spectrum of the DHVA oscillations and hence the anisotropy of the lithium Fermi surface, then the best resolution was achieved by a signal record containing as many oscillations as possible. In such experiments, 16 400 data points were collected corresponding to about 2000 DHVA oscillations over the field range 12.9–7.9 T. These oscillations had a complex beat structure as illustrated in figure 1. Seven long sweeps of this kind were made. For the determination of the electron effective mass, it was necessary that the field should change little and the field sweep was shortened to include approximately 20 oscillations.

Between long sweeps, the sample was sometimes left at the same orientation, to check reproducibility of data, and sometimes rotated by 10 degrees. The purpose of rotation was to provide a check on the randomness of grain orientation in the dispersion. If the dispersion was truly random in the sense that the volume fraction of lithium contributing to a given DHVA frequency depended only on the fraction of Fermi surface orientations that would give that frequency, then the beat structure and Fourier spectrum should be independent of sample orientation.

3. Results and discussion

Figure 2 shows a Fourier spectrum from experiment Li 51, which yielded 2048 data points in the magnetic field range 12.9–12.6 T, and in which the experimental conditions were optimised for the third harmonic ($r = 3$) of the DHVA effect. The prominent grouping of peaks around the lithium free-electron frequency of 41 250 T are the fundamental frequencies of the lithium Fermi surface. The signal-to-noise ratio at this frequency grouping is 25–50 to 1. Also seen feebly are the second and third harmonics of these frequencies. Another peak grouping appears, as it did in each experiment, at a frequency of about 59 000 T with a clearly identifiable second harmonic. These are thought to be DHVA oscillations characteristic of the $\langle 100 \rangle$ belly orbit of copper and to arise from the polycrystalline copper wire of the pick-up coil. For lack of time this has not been convincingly tested by removing the sample, but the frequency is close to that of the B(100) orbit in copper [13] and the effect has also been observed elsewhere [12]. The fact that they were not due to a time frequency was demonstrated by Fourier analysis of the high and low field halves of data block Li42, which yielded no shift in the frequencies. The possibility that these peaks were DHVA oscillations from the low-temperature martensitic phase of lithium was considered. An increase in the area of this peak grouping relative to that of the fundamental lithium grouping would support this view, since one might envisage that the BCC phase slowly transforms over the week of

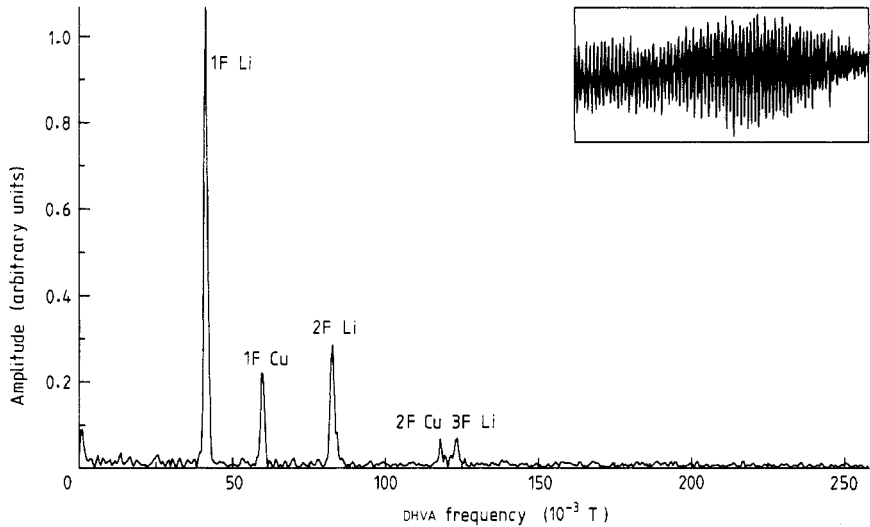


Figure 2. Fourier spectrum of the DHVA effect in lithium. The input data (run Li51) consists of 2048 data points between 12.9 and 12.6 T at a temperature of 20 mk. The experimental conditions were here optimised for the third harmonic ($r = 3$) of the DHVA effect. Some additional peaks, believed to derive from the copper wire of the pick-up coil, are also seen as discussed in the text.

the experiment. No such effect was observed, which is consistent with the fact that these DHVA frequencies derive from the copper pick-up coil.

3.1. Fermi surface anisotropy

Shown in figure 3 are expanded plots of the fundamental lithium frequency grouping from each of seven experiments over an extended field range. Each spectrum is about 1260 T wide and has a sharp cut-off to either side. From the width ΔF of this peak, we can find the overall areal anisotropy $\Delta\mathcal{A}$ of the Fermi surface, since $\Delta F/F_0 = \Delta\mathcal{A}/\mathcal{A}_0$ where F_0 and \mathcal{A}_0 are the free-electron DHVA frequency and extremal cross sectional area, respectively. If each spectrum is regarded as a probability distribution of DHVA frequencies over the Fermi surface, then a picture emerges of one or more substantial peaks below the free-electron frequency F_0 with a tail extending to above F_0 . The differences in detail between the different spectra in figure 3, which are too great to be explained by noise, indicate immediately that the sample is not a perfectly random distribution of orientations. These differences will be quantified and discussed below. However, the width δF of each distribution is insensitive to these fluctuations, and the values of $\Delta F/F_0$ where

$$\Delta F/F_0 = (F_{\max} - F_{\min})/F_0 \quad (11)$$

are summarised in table 1, yielding the value

$$\Delta\mathcal{A}/\mathcal{A}_0 = \Delta F/F_0 = 3.00 \pm 0.02\%. \quad (12)$$

This is substantially higher than the theoretical value of $2.1 \pm 0.4\%$ taken from the two non-local calculations in figure 1 of [6]. We note that, in [7], $\Delta F/F_0$ was found to be $1.5 \pm 0.4\%$ and we suggest that the discrepancy between this and the present result

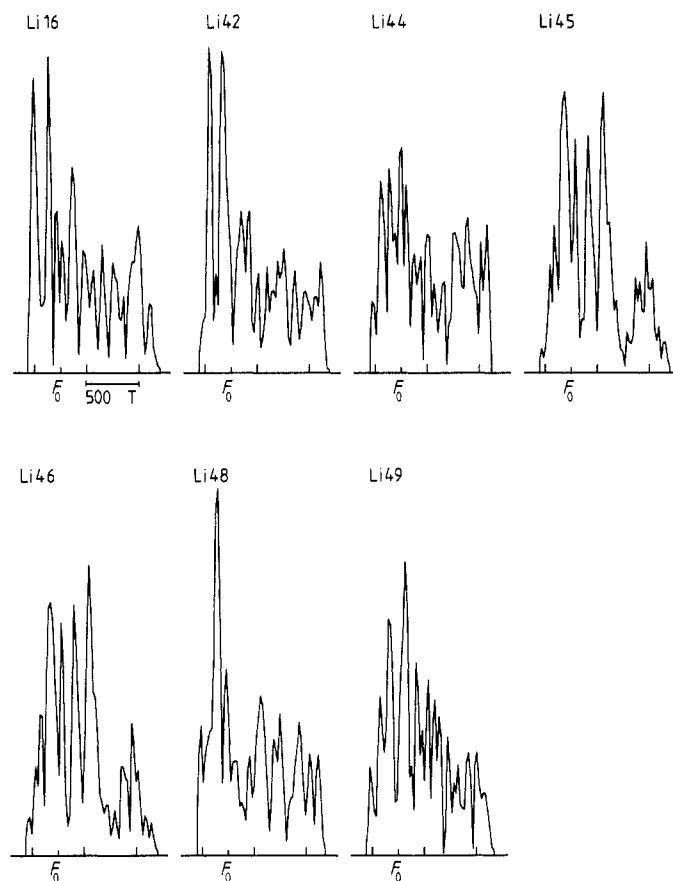


Figure 3. Fourier spectra showing the fine structure of the fundamental term ($r = 1$) of the DHVA effect in a lithium dispersion. Different experiments were made on the same sample placed at different arbitrary orientations to the applied magnetic field. The spectra are normalised to have the same area. F_0 is the calculated free-electron frequency of lithium of 41 250 T.

Table 1. Summary of the width ΔF of the DHVA frequency distribution normalised by the free-electron value $F_0 = 41\,250$ T, as measured in seven experiments. The mean value of $3.00 \pm 0.02\%$ provides the best estimate of the areal anisotropy of the Fermi surface of lithium.

Run	$\Delta F/F_0$ (%)
Li 16	3.08 ± 0.04
Li 42	3.02 ± 0.04
Li 44	2.84 ± 0.08
Li 45	3.02 ± 0.04
Li 46	3.08 ± 0.04
Li 48	2.98 ± 0.08
Li 49	2.98 ± 0.04
Mean	3.00 ± 0.02

arises from the method used in [7] to determine ΔF . This was obtained as the inverse of the field interval between adjacent maxima in the beat envelope of the DHVA oscillations. With the lower fields and limited field range then available the signal-to-noise ratio was only 5 to 1. Some peaks in the envelope may have been lost, effectively reducing the measured ΔF .

For the radial anisotropy δ , we find from the two non-local calculations in figure 2 of [6] that $\delta = 3.3 \pm 0.6\%$. The large errors attached to these theoretical values of $\Delta\mathcal{A}/\mathcal{A}_0$ and δ arise from the errors in the non-local self-energy approximations made in the density functional calculations [6]. These errors are responsible for the differences between the two non-local calculations in both figure 1 and figure 2 in [6]. However, the areal anisotropies in figure 1 in [6] are calculated from the radial anisotropies displayed in figure 2 in [6] using an inversion scheme that introduces further error of less than 1%. Hence, by calculating the ratio $(\Delta F/F_0)/\delta$ for each of the non-local curve pairs in figures 1 and 2 in [6] and taking the mean, we find that the calculations in [6] yield, with low error, $\Delta F/\delta = 0.62 \pm 0.04$. If we make the *assumption* that the same ratio obtains to the experimentally determined areal anisotropy, then the experiment yields

$$\delta = 4.8 \pm 0.3\%. \quad (13)$$

This result is significantly higher than the prediction in [6] and also higher than the positron annihilation result in [8].

We note that this experimental result is not subject, as is that in [7], to assumptions of invariability over the Fermi surface of Dingle temperature, effective mass or spin factor g as we are here only concerned with the overall width ΔF of the frequency distributions in figure 3. The measured anisotropy will be too small only in the unlikely event that the product gm_c is such that the cosine term in equation (1) vanishes in one or other of the *edge* channels in the lithium fundamental grouping of the Fourier spectrum. In this case, δ in equation (13) would represent a lower limit to the anisotropy.

We have considered the possibility that hydrostatic, or even non-hydrostatic, pressures may result, because the lithium grains adhere to the wax matrix. This possibility was first raised in [14] but was not found to be of importance in the experiments in [15] on oil-enclosed potassium samples. We note that in figure 3 the lower edge of the frequency distribution is both sharply defined and also close to F_0 . Additionally, in similar experiments on a dispersion of sodium in wax [7], the Fermi surface derived was found to be in good agreement with that obtained from experiments on a single crystal. We conclude from these observations that the influence of the encapsulating medium is negligible in the present experiments.

3.2. Effects of non-randomness of the sample

Whilst the Fourier spectra reproduced in figure 3 for seven different experiments yield values for the width $\Delta F/F_0$ of the DHVA frequency distribution which are in good agreement (see table 1), they display significant differences in detail in their internal structures. The normalised amplitudes in a given channel are seen to vary by as much as ± 15 – 20% . We believe that this arises because our samples do not constitute a statistically random distribution of lithium particles, in the sense that the volume fraction of particles whose crystallographic orientation lies in a certain range with respect to some arbitrary axis is independent of the orientation.

We note that experiments Li45 and Li46 in figure 3, which were done consecutively within a period of about 2 h *without* change in sample orientation, are identical to within

experimental error. When, however, the two experiments Li48 and Li49 were performed consecutively but at *different* orientations of the sample, then significant differences in the internal structures of the Fourier spectra appear. This is strong evidence for non-randomness of the sample. Of particular interest are the pair of experiments Li44 and Li45 which, whilst at the same orientation, were separated in time by 3 days, the sample being maintained throughout at less than 4.2 K. We have considered whether the differences in their DHVA frequency spectra might in this case arise from a modification of the sample brought about by a slow martensitic transformation. We consider this to be unlikely because the total areas of the two spectra Li44 and Li45 in figure 3 are the same (10.6 ± 0.1 arbitrary units by integration). The Fermi surface in the transformed 9R structure is not expected to be recognisable as a slightly distorted sphere as for BCC lithium. The loss of cubic symmetry leads to a shortening of the Brillouin zone along [100] and to a Fermi surface which extends into at least two zones. A consideration of this model indicates that transformed particles are effectively removed from contributing in the frequency range of BCC lithium (i.e. close to F_0). This conclusion, that martensitic transformation is inhibited in the present experiments, is also supported by the low-temperature x ray experiments in [7]. It is probable that, owing to temperature cycling and mechanical vibrations, the sample has rotated in the probe between experiments Li44 and Li45.

It is evident that whether a finite number N of lithium grains is statistically random in the present experiment will depend on several factors, including N , the size distribution $Q(d)$, d being the grain diameter, and the Fermi surface distortion as measured by $P(F/F_0)$. In the following, we attempt to quantify the effects of the inevitable non-randomness in a finite sample on the measured DHVA frequency distribution.

An additional factor included is that each grain of volume V contributes only an effective volume V_{eff} , which is less than V by the volume of an outer shell of thickness one cyclotron radius. In the semi-classical model, we assume that collisions with the surface effectively remove the electrons from contributing coherently to the DHVA effect. Let V_{tot} be the total volume of lithium. We wish to calculate the relative error $\Delta P(F)/P(F)$ in the channel F to $F + \delta F$ of the probability distribution $P(F)$.

In channel F to $F + \delta F$ the number of grains with diameters in the range d to $d + \delta d$ is

$$n_{F,d} = NP(F)Q(d) \delta F \delta d.$$

The error in $n_{F,d}$ is then

$$\sigma(n_{F,d}) = [NP(F)Q(d) \delta F \delta d]^{1/2}$$

and so the corresponding error arising from fluctuation in volume from sample to sample is

$$\sigma(V_{F,d}) = [NP(F)Q(d) \delta F \delta d]^{1/2} V_{\text{eff},d}$$

so

$$\sigma^2(V_{\text{eff},d}) = NP(F)Q(d)V_{\text{eff},d}^2 \delta F \delta d.$$

Summing over all particle sizes gives

$$(\Delta V_{\text{eff},F})^2 = \sum_d \sigma^2 V_{\text{eff},d}.$$

Then

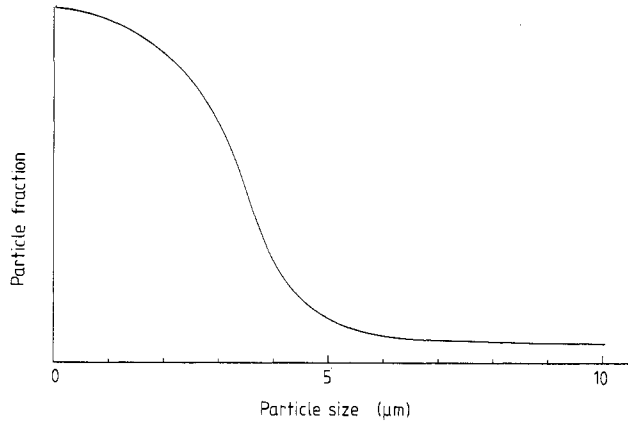


Figure 4. The distribution function of the diameters of the lithium particles.

$$\begin{aligned} \Delta V_{\text{eff } F} / V_{\text{eff } F} &= \left(\sum_d \sigma^2(V_{\text{eff } F, d}) \right)^{1/2} / P(F) V_{\text{eff tot}} \\ &= [NP(F) \delta F]^{1/2} \left(\sum_d Q(d) V_{\text{eff } d}^2 \delta d \right)^{1/2} / P(F) V_{\text{eff tot}} \end{aligned}$$

but $N = V_{\text{eff tot}} / \bar{V}_{\text{eff}} = V_{\text{Tot}} / \bar{V}$ and $\sum_d Q(d) V_{\text{eff } d}^2 \delta d = \bar{V}_{\text{eff}}^2$ so that we have finally

$$\begin{aligned} \Delta V_{\text{eff } F} / V_{\text{eff } F} &= [1/P(F)^{1/2}] [(1/V_{\text{Tot}}) (\bar{V}_{\text{eff}}^2 / \bar{V}_{\text{eff}}^2) \bar{V}]^{1/2} \\ &= \Delta P(F) / P(F) \end{aligned} \quad (14)$$

where $Q(d)$ is such that, if the larger particles dominate the behaviour as here, then $V_{\text{eff}} \approx V$ and equation (14) becomes

$$\Delta P(F) / P(F) = \{1/[NP(F)]^{1/2}\} (V_{\text{rms}} / V). \quad (15)$$

Some of the lithium paste was examined under a microscope to determine the size distribution of grains. This distribution, shown in figure 4, was then modelled and used in a computer program to calculate the fluctuations in amplitude expected in the Fourier spectra using equation (14). It was found that, if the tail of the size distribution was extended to allow a substantial number of grains in the diameter range 100–200 μm , then the fluctuations were of the order of 30–40%. Although no grains larger than 100 μm were noticed in the paste under the microscope, it is entirely possible that the sample itself may have held such grains.

3.3. The probability distribution of DHVA frequencies

If we assume that the fluctuations observed in the distribution of DHVA frequencies between different samples, or equivalently at different orientations of the same sample, are plausibly accounted for by the effect of non-randomness, as discussed above, then the best experimental value for the frequency distribution will be the mean of the normalised distributions in figure 3. This has been calculated and is as shown in figure

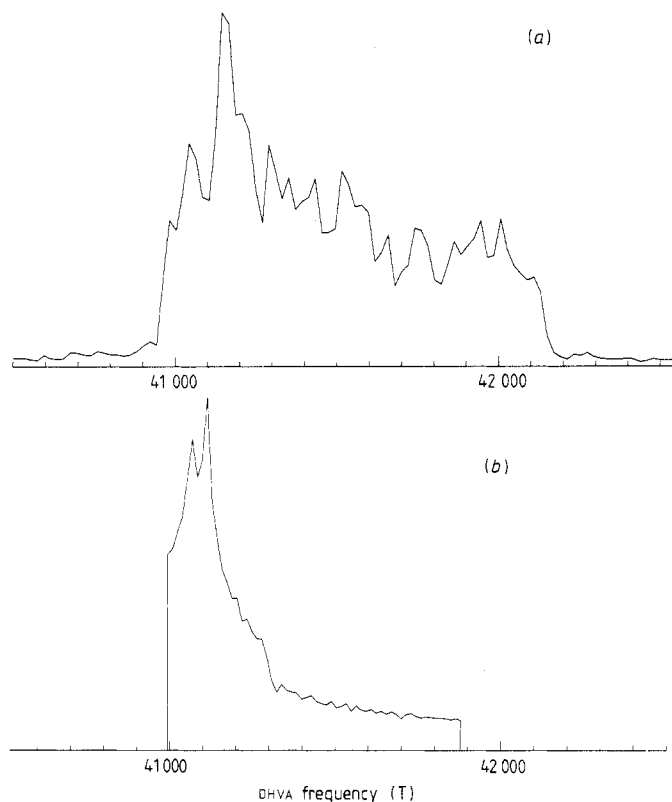


Figure 5. Fourier spectrum showing the fine structure of the fundamental term ($r = 1$) of the DHVA effect in a lithium dispersion: (a) experimental result, being the average of the seven experiments depicted in figure 3; (b) theoretical curve calculated using the non-local model in [6] for the Fermi surface of lithium.

5(a). In general, however, this measured distribution will be systematically in error of the true distribution $P(F)$ because of variations in m_c , T_D and g -factor over the Fermi surface.

In [6] a variation was found in the cyclotron band mass over the Fermi surface of about 20% with the orbital values $m_{111} > m_{100} > m_{110}$ which at 12.9 T produces a variation in DHVA amplitude of about 50%. The high-frequency tail due to the $\langle 110 \rangle$ extremal cross sections would be decreased, while the low-frequency peaks from cross sections in the neighbourhood of the $\langle 100 \rangle$ plane would be enhanced. We assume here that the electron-phonon mass enhancement does not alter the sense of the mass anisotropy as calculated in [6].

The variations in T_D and g over the Fermi surface are unknown but they are not expected to vary greatly, in view of the nearly spherical Fermi surface. However, if the product gm_c were to cause the factor $\cos(\pi rS)$ to vanish at some orientations, then the measured probability distribution would be drastically in error at the corresponding frequencies. We expect, however, that $\cos(\pi rS)$ is large over most of the Fermi surface since we saw above that the observed signal amplitude is of the same order as that calculated on the basis of $\cos(\pi rS) = 1$ everywhere. This analysis is subject, in other words, to the same constraints as affected the anisotropy analysis in [7]. For comparison,

we show in figure 5(b) a whole Fermi surface DHVA frequency distribution generated using a nine-term Kubic harmonic expansion fit to the non-local curves of figure 1 in [6]. We see that this and the experimental curve have qualitatively similar forms but that the distribution in [6] has an accentuated low-frequency peak and a less prominent high-frequency tail. It is not possible to draw detailed conclusions from these differences, since they could easily be accounted for by even very small fluctuations over the Fermi surface of the product gm_c in the term $\cos(\pi rS)$.

3.4. Cyclotron effective-mass measurements

Inspection of equation (1) shows that, for a given DHVA frequency at a given field, the variation with temperature in the amplitude of \bar{M} depends only on the cyclotron effective mass m_c^* appropriate to the extremal Fermi surface orbit. Ordinarily, in single-crystal DHVA work, the measured m_c^* would be that corresponding to an average around a single or at most a small finite set of extremal orbits but in the present case the whole of the Fermi surface is accessed at once so the measured m_c^* is an average over the entire surface. It is nevertheless useful to measure m_c^* in order to obtain an estimate of the electron-phonon interaction.

With the sample orientation fixed, a window of 20 DHVA oscillations at a mean field of 12.82 T was recorded at six different temperatures between 20 and about 800 mK. Analysis of the results yielded the value $m_c^*/m_0 = 2.10 \pm 0.06$ which is close to the specific heat mass of 2.2 [16, 17] and significantly higher than the directly comparable DHVA result in [7] where the value 1.86 ± 0.10 was obtained. If we take the non-local band mass of 1.39 from [6], we find $1 + \lambda$ to be 1.51 and, if we take the local band mass of 1.55 from [6], then $1 + \lambda$ is 1.35. The value of $1 + \lambda$ calculated in [18] is about 1.4, in broad agreement with the present results.

Such a value for $1 + \lambda$ highlights an anomalous behaviour of lithium. The formula [19]

$$\ln(1.45 T_c/\theta_D) = -1.04(1 + \lambda)/[\lambda - (1 + 0.62\lambda)\mu^*]$$

where $\mu^* \approx 0.1$ relates λ to superconducting transition temperature T_c and works well for many superconductors. It gives, for lithium, $T_c = 4.3$ K or 0.590 K according to whether we use the non-local or the local band mass to find $1 + \lambda$. In searches down to 6 mK, lithium is not superconducting. Presumably the mass enhancement is not entirely due to the electron-phonon interaction, but electron-electron effects are also present. This point is discussed by Wilkins in [20].

3.5. Determination of the Dingle temperature

The variation in the amplitude of the fundamental ($r = 1$) term of \bar{M} with magnetic field is seen from equation (1) to be determined by the product AI_1 where $A = \alpha(1/H)D(H)K_1$. In this experiment, I_1 is close to unity over the whole field range. Thus a plot of $\ln(A/H^{1/2})$ against $1/H$ should show a linear drop over peaks of the beating envelope, with slope $-\kappa m_c T_D$. If m_c is known, T_D can be determined. The amplitude should first be corrected for the approximately 8% drop in effective sample volume between high and low fields caused by the increase in electron cyclotron radius. From such an analysis, we find, using the above measured value $m_c^* = 2.1 m_0$, that $T_D = 1.0 \pm 0.3$ K, the value used earlier to estimate the signal amplitude.

Over the field range used, the amplitudes of the highest peaks in the envelopes did not always show a linear drop when plotted as above, especially for runs Li46 and Li48. The field range may have been too short for the beats to unfold completely. As with the effective mass, this measurement is a mean value over the entire Fermi surface.

4. Conclusion

DHVA effect oscillations have been observed in a dispersion of lithium grains. The overall areal anisotropy of the lithium Fermi surface has been measured as $3.00 \pm 0.02\%$. This represents the most accurate measurement to date of this parameter. The observed anisotropy is substantially larger than the value $2.1 \pm 0.4\%$ which is predicted by the non-local model in [6]. Whilst the origin of this discrepancy is unclear to us, we note the recent discussion in [21] where attention is drawn to the inequivalence of the Kohn-Sham Fermi surface obtained from density functional theory and the physical Fermi surface, as observed in the present experiment. Of interest also is the radial anisotropy δ . Whilst this has not been measured directly, we can estimate δ using the ratio of δ to $\Delta\mathcal{A}$ found in [6]. We obtain $\delta = 4.8 \pm 0.3\%$ which is significantly higher than the value of $2.8 \pm 0.6\%$ deduced from recent positron annihilation experiments in [8]. Confidence in our estimate is enhanced by the work in [7] where, in an earlier version of this investigation, parallel experiments with dispersions of sodium for which the radial Fermi surface anisotropy is known independently were carried out. It was found that the indirectly measured radial anisotropy for sodium was in good agreement with the accepted value.

A probability distribution of DHVA frequencies over the whole Fermi surface was produced. This is thought to be subject to random errors in amplitude of about 10% but also to less easily characterised systematic errors arising from anisotropies over the Fermi surface of g , m_c and T_D . Comparison with a distribution generated from the non-local model in [6] shows that the two are qualitatively similar. Both have a high-frequency tail and a low-frequency peak, with sharp cut-offs to either side. The electron cyclotron effective mass is measured at 2.10 ± 0.06 in units of the free-electron mass, in good agreement with measurements of electronic specific heats [16, 17].

References

- [1] Smith H G 1987 *Phys. Rev. Lett.* **58** 1228
- [2] Overhauser A W 1984 *Phys. Rev. Lett.* **53**
- [3] Cohen M H and Heine V 1958 *Adv. Phys.* **7** 395
- [4] O'Keefe P M and Goddard III W A 1969 *Phys. Rev. Lett.* **23** 300
- [5] Rasolt M, Nickerson S B and Vosko S H 1975 *Solid State Commun.* **16** 827
- [6] Macdonald A H 1980 *J. Phys. F: Met. Phys.* **10** 1737
- [7] Randles D L and Springford M 1976 *J. Phys. F: Met. Phys.* **6** 1827
- [8] Oberli L, Manuel A A, Sachot R, Descouts P and Peter M 1985 *Phys. Rev. B* **31** 6104
- [9] Gold A V 1968 *Solid State Physics* vol 1 *Electrons in Metals* ed. J F Cochran and R R Haering
- [10] Lifshitz I M and Kosevich A M 1956 *Sov. Phys.-JETP* **2** 636
- [11] Reinders P H P, Springford M, Hilton P, Hilton N and Killoran N 1987 *Cryogenics* **27** 689
- [12] Shoenberg D 1984 *Magnetic Oscillations in Metals* (Cambridge: CUP)
- [13] Poulsen R G, Randles D L and Springford M 1974 *J. Phys. F: Met. Phys.* **4** 981, table 1
- [14] Dugdale J S and Gugan D 1963 *J. Sci. Instrum.* **40** 28
- [15] Templeton I M 1972 *Phys. Rev. B* **5** 3819

- [16] Martin D L 1961 *Proc. R. Soc. A* **263** 378
- [17] Martin D L 1965 *Proc. R. Soc. A* **139** 150
- [18] Grimwall G 1976 *Phys. Scr.* **14** 63
- [19] McMillan W L 1968 *Phys. Rev.* **167** 331
- [20] Springford M (ed.) 1980 *Electrons at the Fermi Surface* (Cambridge: CUP)
- [21] Mearns D 1988 *Phys. Rev. B* **38** 5906